

# Solid state reaction synthesis and photoluminescence properties of Dy<sup>3+</sup> doped NaGd(MoO<sub>4</sub>)<sub>2</sub> phosphor

Lihui Zhang<sup>a</sup>, Haiyang Zhong<sup>a,\*</sup>, Xiangping Li<sup>a</sup>, Lihong Cheng<sup>a</sup>, Li Yao<sup>a</sup>, Jiashi Sun<sup>a</sup>,  
Jinsu Zhang<sup>a</sup>, Ruinian Hua<sup>b</sup>, Baojiu Chen<sup>a,\*\*</sup>

<sup>a</sup> Department of Physics, Dalian Maritime University, Dalian 116026, PR China

<sup>b</sup> College of Life Science, Dalian Nationalities University, Dalian 116600, PR China

Received 10 February 2012; received in revised form 21 February 2012; accepted 21 February 2012

Available online 3 March 2012

## Abstract

Dy<sup>3+</sup> doped NaGd(MoO<sub>4</sub>)<sub>2</sub> phosphors were synthesized by a traditional solid-state reaction route using NH<sub>4</sub>HF<sub>2</sub> as a flux. The influence of calcination temperature on the crystal structure and spectral properties was studied, and the optimum calcination temperature for producing Dy<sup>3+</sup> doped NaGd(MoO<sub>4</sub>)<sub>2</sub> phosphor was experimentally confirmed. The concentration quenching of Dy<sup>3+</sup> fluorescence and excitation-wavelength dependent spectroscopic properties were studied. On the base of both the Van Uitert's and I-H models, the electric dipole–dipole (D–D) interaction was ascribed to be the main physical mechanism responsible for energy transfer between Dy<sup>3+</sup> ions. It was also discovered that the color coordinates of the Dy<sup>3+</sup> doped NaGd(MoO<sub>4</sub>)<sub>2</sub> phosphor depends on the Dy<sup>3+</sup> doping concentration and the excitation wavelength.

© 2012 Elsevier Ltd and Techna Group S.r.l. All rights reserved.

**Keywords:** A. Powders; solid state reaction; B. Spectroscopy; C. Optical properties

## 1. Introduction

Rare earth ions existing in trivalent and divalent states own a great deal of levels and many transitions whose wavelengths covering the region from UV to mid-IR. Up to now, rare earth activated phosphors still attract much attention due to their practical or potential applications in many fields, such as displays, lighting sources, sensing devices and so on [1–4]. Especially, the introduction of trivalent rare earth ions as luminescent centers into matrices is considered as an excellent approach for preparing the superior luminescent materials [5–9], thus, trivalent rare earth ions doped phosphors have been extensively studied. Much attention has been paid to the trivalent dysprosium ion (Dy<sup>3+</sup>) [10–13], because Dy<sup>3+</sup> has two principal bands in its emission spectrum, viz. the intense blue and yellow emissions corresponding to the <sup>4</sup>F<sub>9/2</sub> → <sup>6</sup>H<sub>15/2</sub> and <sup>4</sup>F<sub>9/2</sub> → <sup>6</sup>H<sub>13/2</sub> transitions centered at around 480 and 575 nm, respectively [14–20]. Amongst these two emissions, the yellow

one is hypersensitive and its emission intensity strongly depends on the local crystal field environment where the Dy<sup>3+</sup> is located, thus the emission color of the Dy<sup>3+</sup> doped phosphors can be tuned by properly designing the host. And if the emission intensities of yellow and blue ones are approximately identical, the white light can be achieved. Meanwhile, the white light coming from Dy<sup>3+</sup> singly doped solo-host is also preferable in the practical applications.

Usually, the phosphors performance can be influenced by the host materials, thus choosing a suitable host for specific rare earth ion is extremely important. In recent years, rare earth ions doped phosphors based on many host materials such as molybdates [21], tungstates [22,23], vanadates [24] and aluminates [25,26], etc. were widely studied because of their long longevity, low cost, and excellent physical and chemical stability [27]. Among these hosts, molybdates exhibit a large number of different crystal structures containing the same or different elements, and attract growing interest due to their strong and broad charge transfer absorption band in near ultraviolet region and due to possible efficient energy transfer from molybdate groups to the rare earth doping centers [28], enabling them to be excellent host materials for rare earth ions doped phosphors [29–32].

\* Corresponding author. Tel.: +86 411 84728909; fax: +86 411 84728909.

\*\* Corresponding author.

E-mail address: [chenmbj@sohu.com](mailto:chenmbj@sohu.com) (B. Chen).

In this study, the optimal calcination temperature and doping concentration of  $\text{Dy}^{3+}$  were also confirmed.  $\text{NaGd}(\text{MoO}_4)_2$  phosphors with different concentrations of  $\text{Dy}^{3+}$  were successfully synthesized via a conventional solid state reaction method, and their crystal structure was examined using X-ray diffraction (XRD). The luminescent properties of the samples were analyzed via fluorescence spectroscopy. The electric dipole–dipole interaction between  $\text{Dy}^{3+}$  is confirmed through the analysis of luminescent concentration quenching and fluorescence decay. The chromatic properties of phosphors were also investigated.

## 2. Experimental details

### 2.1. Chemicals

Gadolinium oxide ( $\text{Gd}_2\text{O}_3$ , 99.99%), dysprosium oxide ( $\text{Dy}_2\text{O}_3$ , 99.99%), molybdenum oxide ( $\text{MoO}_3$ , 99.99%) and sodium carbonate ( $\text{NaCO}_3$ , 99.9%) were used as starting materials.  $\text{NH}_4\text{HF}_2$  with purity of 99.99% was employed as flux to improve the chemical reaction.

### 2.2. Sample synthesis

The  $\text{NaGd}(\text{MoO}_4)_2\cdot\text{Dy}^{3+}$  phosphors were synthesized via a conventional solid-state reaction method. According to a certain stoichiometric ratio, the starting materials were weighed and grinded thoroughly in an agate mortar. Then the mixtures were put into alumina crucibles and calcined in a muffle furnace for 4 h at various temperatures from 700 to 1100 °C. It was found that when the temperature is 1100 °C, the obtained resultant displays maximum emission intensity and good crystallinity, implying that 1100 °C is the optimal temperature. A series of phosphors  $\text{NaGd}(\text{MoO}_4)_2$  with various concentrations of  $\text{Dy}^{3+}$  (0.2%, 0.5%, 1%, 3%, 7%, 10%, 20% in molar) was prepared at 1100 °C.

### 2.3. Sample characterization

The crystal structure of the samples was identified with a Shimadzu X-ray diffractometer (XRD)-6000 operating at 40 kV and 100 mA with Cu  $\text{K}\alpha_1$  radiation ( $\lambda = 1.5406 \text{ \AA}$ ). The excitation and emission spectra of the phosphors were recorded with a Hitachi F-4600 fluorospectrometer equipped with a 150 W Xe lamp as excitation source. Before surveying the spectrum, a calibration procedure was run by using the standard accessories offered by the manufacturer. All the measurements were performed at the room temperature.

## 3. Results and discussion

### 3.1. Effects of calcination temperature on the crystal structure and luminescence

#### 3.1.1. Effect of calcination temperature on crystal structure

The calcination temperature for solid-state reaction is an important factor affecting the crystal structure of the resultants,

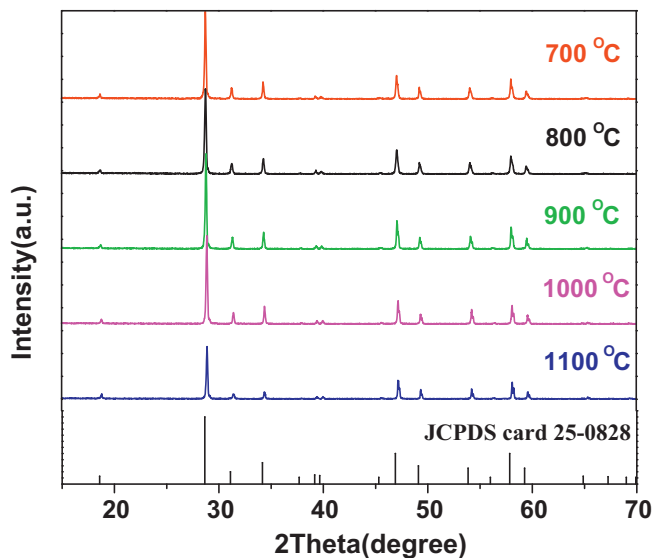


Fig. 1. XRD patterns of 1 mol%  $\text{Dy}^{3+}$  doped  $\text{NaGd}(\text{MoO}_4)_2$  prepared at different temperatures.

thus it should be optimized in order to obtain high performance phosphors. In this study, we prepared a set of  $\text{NaGd}(\text{MoO}_4)_2$  phosphors doped with the same  $\text{Dy}^{3+}$  concentration of 1 mol% at different temperatures from 700 to 1100 °C. The XRD patterns for the  $\text{NaGd}(\text{MoO}_4)_2\cdot 1 \text{ mol\% Dy}^{3+}$  prepared at different calcination temperatures are shown in Fig. 1. The XRD patterns indicate that the calcination temperature in the region of 700–1100 °C has little influence on the structures of the resultant phosphors. By comparing with the JCPDS card no. 25-0828, it can be found that the patterns of the prepared samples are consistent well with tetragonal  $\text{NaGd}(\text{MoO}_4)_2$ . No additional diffraction peaks corresponding to other compounds are observed in the patterns, which indicates that the prepared samples are pure phased  $\text{NaGd}(\text{MoO}_4)_2$ . From the above results it can be concluded that the  $\text{NaGd}(\text{MoO}_4)_2\cdot\text{Dy}^{3+}$  phosphors can be obtained in a wide temperature region at least from 700 to 1100 °C.

#### 3.1.2. Dependence of spectral properties on calcination temperature

In order to investigate the influence of calcination temperature on the luminescent properties, the excitation and emission spectra for all the samples prepared at various temperatures were measured under the same experimental conditions. Fig. 2 shows the excitation spectra of  $\text{NaGd}(\text{MoO}_4)_2$  phosphors with 1 mol%  $\text{Dy}^{3+}$  prepared at different reaction temperatures (700–1100 °C) by monitoring 577 nm emission corresponding to the  $^4\text{F}_{9/2} \rightarrow ^6\text{H}_{13/2}$  transition of  $\text{Dy}^{3+}$ . The excitation spectra consist of two parts, a weak broad band centered at 270 nm and a set of sharp lines. The weak broad excitation band originates from the charge-transfer band (CTB) of Mo–O, thus implying a very weak energy transfer from  $\text{MoO}_4^{2-}$  to  $\text{Dy}^{3+}$  ions. The set of sharp lines ranging from 305 to 500 nm is due to the f–f transitions of  $\text{Dy}^{3+}$  from the ground state  $^6\text{H}_{15/2}$  to the excited state  $^4\text{P}_{7/2}$ ,  $^4\text{P}_{3/2}$ ,  $^4\text{F}_{7/2}$ ,  $^4\text{G}_{11/2}$ ,  $^4\text{H}_{11/2}$  and  $^4\text{F}_{9/2}$ , respectively [10]. From the excitation spectra

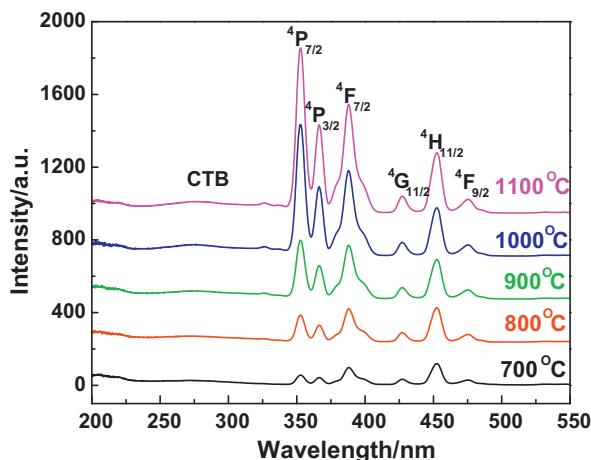


Fig. 2. Excitation spectra of NaGd(MoO<sub>4</sub>)<sub>2</sub>: 1 mol% Dy<sup>3+</sup> phosphors prepared at different temperatures by monitoring the emission at 577 nm.

we can see that the f–f transition intensities monotonously increase with increasing the calcination temperature.

Fig. 3 shows the emission spectra for the phosphors with 1 mol% Dy<sup>3+</sup> prepared at different calcination temperatures excited by 270 nm corresponding to the charge transition of Mo–O. A broad band accompanying with two sharp lines is observed in the emission spectra. The broad band centered at 400 nm can be assigned to the Mo–O charge transfer transition in NaGd(MoO<sub>4</sub>)<sub>2</sub> host. Two sharp line emissions peaking at 483 and 577 nm can be attributed to the transitions of <sup>4</sup>F<sub>9/2</sub> → <sup>6</sup>H<sub>15/2</sub> (blue) and <sup>4</sup>F<sub>9/2</sub> → <sup>6</sup>H<sub>13/2</sub> (yellow) of Dy<sup>3+</sup>, respectively. In addition, it can be found that the emission intensities of Dy<sup>3+</sup> in the NaGd(MoO<sub>4</sub>)<sub>2</sub> phosphors increase with the increase of calcination temperature. This fact means that higher temperature is beneficial to the synthesis of NaGd(MoO<sub>4</sub>)<sub>2</sub>:Dy<sup>3+</sup> phosphors. Meanwhile, the existence of Dy<sup>3+</sup> emission peaks in the emission spectra measured by

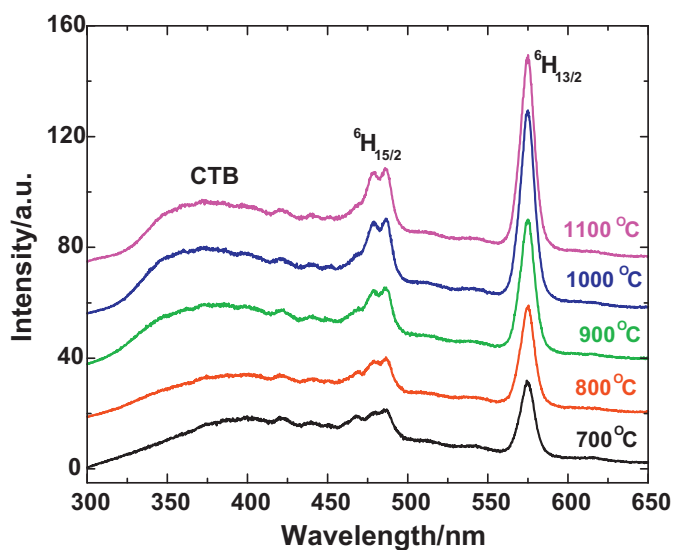


Fig. 3. Fluorescent emission spectra of NaGd(MoO<sub>4</sub>)<sub>2</sub>: 1 mol% Dy<sup>3+</sup> phosphors prepared at different temperatures upon 270 nm excitation.

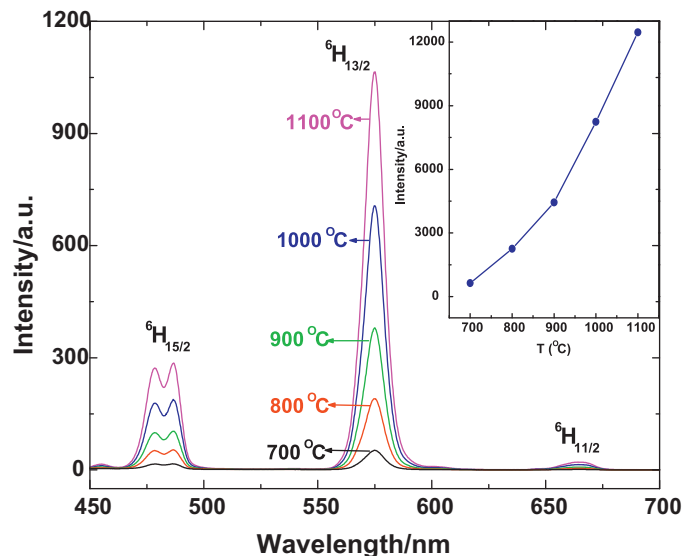


Fig. 4. Fluorescent emission spectra of NaGd(MoO<sub>4</sub>)<sub>2</sub>: 1 mol% Dy<sup>3+</sup> phosphors prepared at different temperatures upon 353 nm excitation.

exciting the Mo–O charge transfer band indicates that the energy transfer from host NaGd(MoO<sub>4</sub>)<sub>2</sub> to Dy<sup>3+</sup> takes place.

Fig. 4 shows the emission spectra for the phosphors doped with 1 mol% Dy<sup>3+</sup> prepared at different calcination temperatures when excited by 353 nm corresponding to intrinsic absorption of Dy<sup>3+</sup>. Two intense emissions centered at 483 (blue) and 577 (yellow) nm, and a weak emission centered at 665 (red) nm corresponding to transitions from <sup>4</sup>F<sub>9/2</sub> to <sup>6</sup>H<sub>J</sub> (*J* = 15/2, 13/2 and 11/2) are observed. However, the emission peak belonging to charge transfer transition of NaGd(MoO<sub>4</sub>)<sub>2</sub> host as has detected under 270 nm excitation is not observed in Fig. 4, thus indicating there is no such an energy transfer from Dy<sup>3+</sup> to Mo–O charge transfer state when the phosphors are excited by 353 nm. The insert of Fig. 4 shows the relationship between the integrated emission intensity of <sup>4</sup>F<sub>9/2</sub> → <sup>6</sup>H<sub>13/2</sub> transition and the calcination temperature. It is seen that the integrated emission intensity increases with the increase of the calcination temperature. From above results it can be deduced that higher calcination temperature is required for obtaining the NaGd(MoO<sub>4</sub>)<sub>2</sub>:Dy<sup>3+</sup> with intense luminescence. However, we found that when the calcination temperature was higher than 1100 °C, the resultant become solid conglomeration and could not be steamrolled easily. Therefore, the calcination temperature of 1100 °C was adopted for preparing the NaGd(MoO<sub>4</sub>)<sub>2</sub> phosphors with various Dy<sup>3+</sup> concentrations.

### 3.2. Concentration effects on the crystal structure and luminescence of NaGd(MoO<sub>4</sub>)<sub>2</sub>:Dy<sup>3+</sup>

#### 3.2.1. Crystal structure of the phosphors with different concentrations of Dy<sup>3+</sup>

Doping concentration of rare earth ions activated phosphors is one of the important factors influencing luminescent performance. In order to inspect the effect of Dy<sup>3+</sup> doping concentration on the spectroscopic property, the NaGd(MoO<sub>4</sub>)<sub>2</sub> phosphors doped with various concentrations of Dy<sup>3+</sup> were

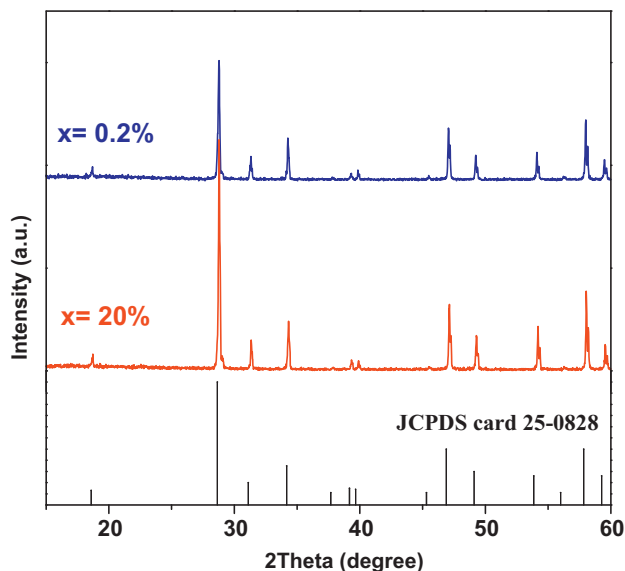


Fig. 5. XRD patterns of the samples prepared at 1100 °C with different concentration of Dy<sup>3+</sup>.

prepared at calcination temperature of 1100 °C. For the sake of validating the effect of doping concentration on the resultant crystal structure, the XRD patterns for the samples doped with low (0.2%) and high (20%) concentrations of Dy<sup>3+</sup> were measured and are shown in Fig. 5 where the standard diffraction pattern plotted by using the data reported in JCPDS card no. 25-2808 is also given. By comparing the XRD patterns of the studied samples with the standard pattern, it can be found that there is no any additional diffraction peak other than those from tetragonal phase NaGd(MoO<sub>4</sub>)<sub>2</sub>, thus implying that the doping concentration did not affect the product form at present doping level.

### 3.2.2. Dependence of spectral properties on concentrations of Dy<sup>3+</sup>

Fig. 6 shows the excitation spectra of NaGd(MoO<sub>4</sub>)<sub>2</sub> phosphors with different doping concentrations by monitoring 577 nm emission corresponding to the <sup>4</sup>F<sub>9/2</sub> → <sup>6</sup>H<sub>13/2</sub> transition of Dy<sup>3+</sup> under the same experimental conditions. The arrow line indicates the increase of Dy<sup>3+</sup> doping concentration. Each excitation spectrum consists of the Mo–O charge transfer band centered at 270 nm and the f–f transitions of Dy<sup>3+</sup> originating from the ground state <sup>6</sup>H<sub>15/2</sub> to the excited state <sup>4</sup>P<sub>7/2</sub>, <sup>4</sup>P<sub>3/2</sub>, <sup>4</sup>F<sub>7/2</sub>, <sup>4</sup>G<sub>11/2</sub>, <sup>4</sup>H<sub>11/2</sub> and <sup>4</sup>F<sub>9/2</sub>, respectively. It is also observed that with the increase of Dy<sup>3+</sup> concentration the excitation peak intensities of f–f transitions increase first, and then decrease. This fact means that the concentration quenching occurs. Additionally, the Mo–O CTB intensity is weak and changes slightly with the Dy<sup>3+</sup> concentration, indicating the energy transfer from MoO<sub>4</sub><sup>2−</sup> to Dy<sup>3+</sup> is inefficient.

Fig. 7 shows the emission spectra of the phosphors with different concentrations of Dy<sup>3+</sup> excited by 270 nm measured under the same experimental conditions. The arrow line indicates the increase of Dy<sup>3+</sup> doping concentration. Each spectrum displays an overlap of a broad band, two strong narrow emission peaks and one weak peak. The broad band centered at about

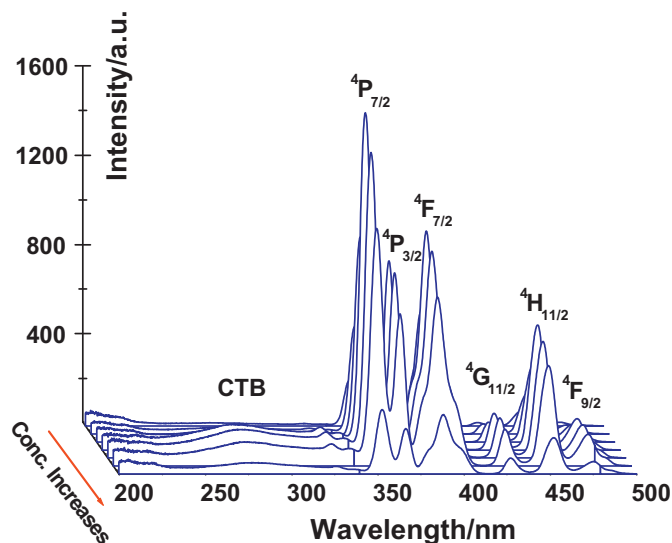


Fig. 6. Excitation spectra of NaGd(MoO<sub>4</sub>)<sub>2</sub> phosphors with different Dy<sup>3+</sup> concentrations by monitoring the emission at 577 nm.

400 nm originates from the charge-transfer band (CTB) of Mo–O. Two principal and intensive emission peaks centered at 483 and 577 nm can be assigned to <sup>4</sup>F<sub>9/2</sub> → <sup>6</sup>H<sub>15/2</sub> and <sup>4</sup>F<sub>9/2</sub> → <sup>6</sup>H<sub>13/2</sub> transitions of Dy<sup>3+</sup>, the weak emission centered at 665 nm can be ascribed to <sup>4</sup>F<sub>9/2</sub> → <sup>6</sup>H<sub>11/2</sub> transition. Moreover, it can also be found that the luminescent properties strongly depend on the doping concentrations. When the doping concentration increases up to 7 mol%, the intensity for each narrow spectral line becomes strongest and then slowly decreases with further increase of Dy<sup>3+</sup> concentrations. The concentration quenching is caused by the cross relaxations between Dy<sup>3+</sup> ions [33].

Fig. 8 depicts the emission spectra of the phosphors with various Dy<sup>3+</sup> doping concentrations under 350 nm excitation. The arrow line indicates the direction following which the Dy<sup>3+</sup> doping concentration increases. It is found that three emission peaks centered at 483, 577 and 664 nm corresponding to <sup>4</sup>F<sub>9/2</sub> → <sup>6</sup>H<sub>15/2</sub>, <sup>4</sup>F<sub>9/2</sub> → <sup>6</sup>H<sub>13/2</sub> and <sup>4</sup>F<sub>9/2</sub> → <sup>6</sup>H<sub>11/2</sub> are

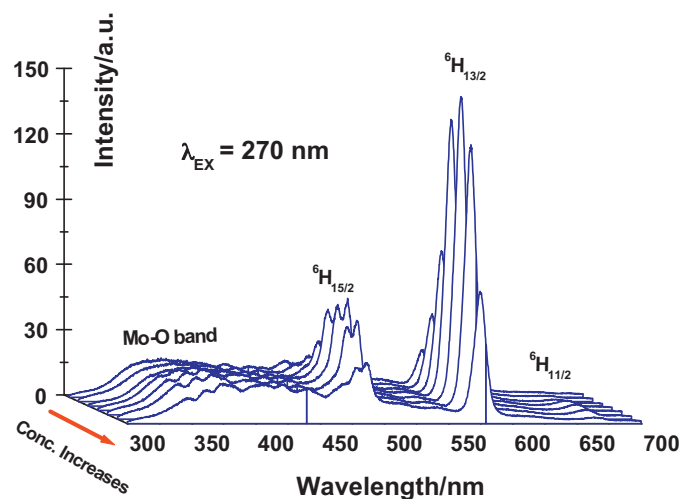


Fig. 7. Fluorescent emission spectra of NaGd(MoO<sub>4</sub>)<sub>2</sub> phosphors with different Dy<sup>3+</sup> concentrations upon 270 nm excitation.

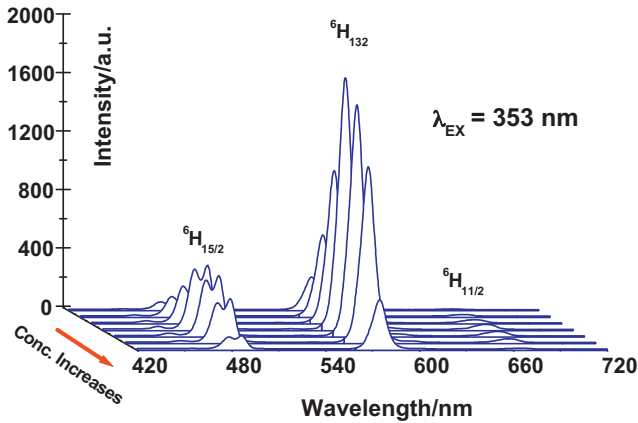


Fig. 8. Fluorescent emission spectra of NaGd(MoO<sub>4</sub>)<sub>2</sub> phosphors with different Dy<sup>3+</sup> concentrations upon 353 nm excitation.

observed in each sample. Amongst these three emissions the yellow one is most intense, and the intensity of each emission increases initially and reaches its maximum at doping concentration of 7 mol%, and then decreases with continuously increasing Dy<sup>3+</sup> concentration. From these experimental results it can be concluded that the optimum doping concentration of Dy<sup>3+</sup> in NaGd(MoO<sub>4</sub>)<sub>2</sub> phosphor for achieving maximum emission intensity is around 7 mol%. When the doping concentration of Dy<sup>3+</sup> is higher than the optimum value, the fluorescence of Dy<sup>3+</sup> will be self-quenched via cross relaxation processes [33].

In order to study the concentration quenching behavior of Dy<sup>3+</sup> fluorescence, the integrated emission intensities of <sup>4</sup>F<sub>9/2</sub> → <sup>6</sup>H<sub>13/2</sub> transition of Dy<sup>3+</sup> for the concentration-varied samples were calculated from the emission spectra in Figs. 7 and 8. It should be mentioned that in the calculations the broad band emission of MoO<sub>4</sub><sup>2-</sup> was excluded when using the spectral data shown in Fig. 7. Fig. 9 shows the concentration dependence of integrated emission intensities of <sup>4</sup>F<sub>9/2</sub> → <sup>6</sup>H<sub>13/2</sub>

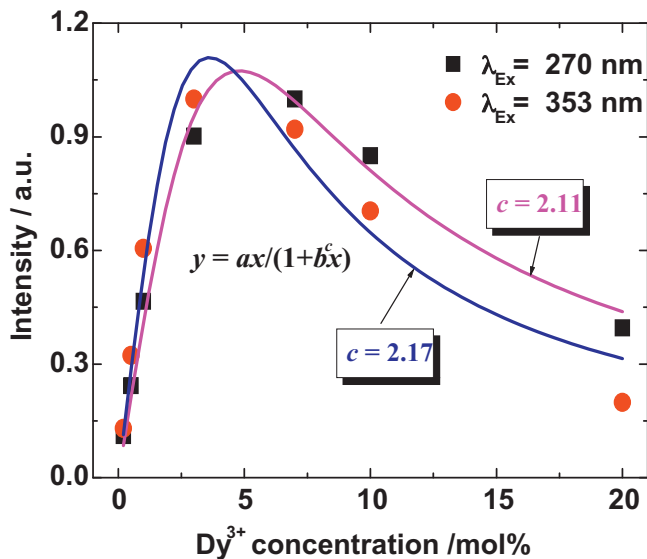


Fig. 9. Dependence of integrated emission intensity on the doping concentration of Dy<sup>3+</sup> excited at 270 and 353 nm.

transition for both the cases of 270 and 353 nm excitations. It can be found that the change of emission intensity with Dy<sup>3+</sup> concentration follows a very similar trend, and the maximum emission intensity can be obtained when Dy<sup>3+</sup> concentration is around 7 mol% in the cases of different excitation.

Van Uitert has investigated on the concentration quenching behavior of doping centers and developed an expression for the relationship between the luminescent intensity and the doping concentration of luminescent center, which can be expressed through the following equation [34]:

$$I(c) = \frac{C}{K[1 + \beta C^{Q/3}]} \quad (1)$$

where  $C$  is doping concentration of rare earth ion;  $K$  and  $\beta$  are constants for a certain system;  $Q$  represents the interacting type between rare earth ions,  $Q = 6, 8$  or  $10$ , indicating the electric dipole–dipole (D–D), electric dipole–quadrupole (D–Q), or electric quadrupole–quadrupole (Q–Q) interactions, respectively. In order to study on the physical mechanism of the interaction between Dy<sup>3+</sup> ions, a simplified mathematical form of Eq. (1),  $y = ax/(1 + bx^c)$ , was used to fit the experimental data in Fig. 9. The solid lines in Fig. 9 show the fitting curves. It can be seen that Eq. (1) fits well with the experimental results, thus indicating that Van Uitert's model can explain well the concentration quenching behavior. From the fitting processes the  $c$  values were derived to be 2.11 and 2.17, respectively, for the cases of 270 and 353 nm excitation. This means that obtained  $Q$  in Eq. (1) are very close to the theoretical value of 6 for D–D interaction, which is in a good agreement with the conclusion derived from the analysis on the energy transfer between Dy<sup>3+</sup> in our previous work [35].

In order to further study on the energy transfer between Dy<sup>3+</sup> the fluorescent decay curve for the highly doped NaGd(MoO<sub>4</sub>)<sub>2</sub> with 10% Dy<sup>3+</sup> was measured under 353 nm excitation by monitoring 577 nm emission. The dotted solid-squares show the experimental data in a semi-log coordinates system where the straight line exhibits the linear fitting to the fluorescence decay data. It can be seen that the fluorescence decay of <sup>4</sup>F<sub>9/2</sub> level of Dy<sup>3+</sup> deviates far from the monoexponential function, which implies that the 577 nm fluorescence is quenching by the energy transfer process [35]. Inokuti and Hirayama have pointed out that in the case of electric multipole interaction between luminescent centers the fluorescence decay of donor obeys following equation [36] which is known as I-H model:

$$I(t) = I_0 \exp \left[ -\frac{t}{\tau_0} - \alpha \left( \frac{t}{\tau_0} \right)^{3/s} \right] \quad (2)$$

where  $\tau_0$  is the intrinsic lifetime of donor,  $I(0)$  is the intensity at time  $t = 0$ ,  $I(t)$  is the luminescence intensity at time  $t$ ,  $\alpha$  is a parameter containing the energy transfer probability, and  $s$  has the same meaning as the aforementioned  $Q$  in Eq. (1). Here,  $s = 6, 8$  or  $10$  for D–D, D–Q, or Q–Q interactions, respectively. Eq. (2) was fitted to the experimental data, and from the fitting process the value of  $s$  was derived to be about 4.8. Though this value is smaller than the theoretical value 6, the D–D interaction between



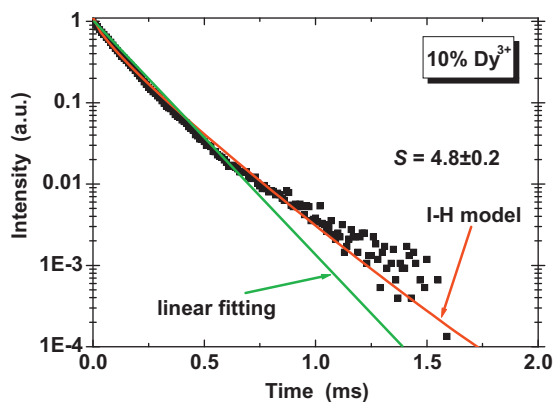


Fig. 10. Fluorescent decays for the phosphor doped with 10 mol%  $\text{Dy}^{3+}$ .

$\text{Dy}^{3+}$  can be confirmed to be dominant in the energy transfer process between  $\text{Dy}^{3+}$  (Fig. 10).

### 3.3. Influence of $\text{Dy}^{3+}$ concentration on the color coordinates

Color coordinates are important factor for evaluating phosphor's performance. The color coordinates for all the samples were calculated based on the Commission Internationale de l'Eclairage (CIE) 1931 standards according to the intensity-calibrated emission spectra shown in Figs. 7 and 8, and the calculation results are revealed in Fig. 11. The open triangle dots and solid circle dots indicate the color coordinates for the phosphors under 270 and 353 nm excitations, respectively. The arrowed curves ABC and abc show the variation trends of the color coordinates with the increase of  $\text{Dy}^{3+}$  doping concentration. It can be seen that the color coordinates are dependent on the excitation wavelength, which is due to the existence of  $\text{MoO}_4^{2-}$  emission when the phosphors with various  $\text{Dy}^{3+}$  concentrations were excited at 270 nm, and in this case the color coordinates change greatly with  $\text{Dy}^{3+}$  doping concentration. However, when the phosphors excited by

353 nm, the color coordinates change slightly with  $\text{Dy}^{3+}$  concentration, this is because of that the spectral profile is almost not varied with  $\text{Dy}^{3+}$  concentration in addition to the change in their emission intensity. The insert in Fig. 11 shows the variation detail of color coordinates for the phosphors under 353 nm excitation. From these results, it can be concluded that dependence of color coordinates on the excitation wavelength and doping concentration of  $\text{Dy}^{3+}$  may be an advantage for the applications in some special fields, for example, indicator devices, lighting of color variation and so on.

## 4. Conclusion

The optimum solid state reaction calcination temperature for preparing  $\text{NaGd}(\text{MoO}_4)_2:\text{Dy}^{3+}$  phosphors was experimentally confirmed to be 1100 °C.  $\text{NaGd}(\text{MoO}_4)_2$  phosphors with various  $\text{Dy}^{3+}$  concentrations were successfully prepared via the modified solid-state reaction. Based on the Van Uitert's mode the concentration quenching behavior of  $\text{Dy}^{3+}$  fluorescence was studied, and the D–D interaction between  $\text{Dy}^{3+}$  ions was found to be the main physical mechanism, which is also in accordance with the conclusion derived from fluorescence dynamic analysis in the framework of I–H model. The study on the chromatic properties of the phosphors indicated that the color coordinates of the  $\text{Dy}^{3+}$  doped phosphors depend on the both the excitation wavelength and the doping concentration of  $\text{Dy}^{3+}$ .

## Acknowledgments

This work was partially supported by NSFC (National Natural Science Foundation of China, Grant nos. 11104024, 50972021, 11104023 and 61078061), Foundation of Education Department of Liaoning Province (Grant no. 2010057), Fundamental Research Funds for the Central Universities (Grant nos. 2011ZD032, 2011ZD033, 2011QN152, 2011JC36 and 2011JC37), and Natural Science Foundation of Liaoning Province (Grant nos. 20111032, 20111031).

## References

- [1] B. Yan, X. Su, Chemical co-precipitation synthesis and photoluminescence of  $\text{LnP}_x\text{V}_{1-x}\text{O}_4:\text{Dy}^{3+}$  ( $\text{Ln} = \text{Gd}, \text{La}$ ) derived from assembling hybrid precursors, *J. Alloys Compd.* 431 (2007) 342–347.
- [2] G. Blasse, B.C. Grabmeyer, *Luminescent Materials*, Springer-Verlag, Berlin, 1994.
- [3] L. Hesselink, S.S. Orlov, A. Liu, A. Akella, D. Lande, R.R. Neurgaonka, Photorefractive materials for nonvolatile volume holographic data storage, *Science* 282 (1998) 1089–1094.
- [4] F.M. Nirwan, T.K. Gundu Rao, P.K. Gupta, R.B. Pode, Studies of defects in  $\text{YVO}_4:\text{Pb}^{2+}$ ,  $\text{Eu}^{3+}$  red phosphor material, *Phys. Status Solidi (a)* 198 (2003) 447–456.
- [5] X. Li, Z. Yang, L. Guan, J. Guo, Y. Wang, Q. Guo, Synthesis and luminescent properties of  $\text{CaMoO}_4:\text{Tb}^{3+}$ ,  $\text{R}^+$  ( $\text{Li}^+$ ,  $\text{Na}^+$ ,  $\text{K}^+$ ), *J. Alloys Compd.* 478 (2009) 684–686.
- [6] T. Kim, S. Kang, Potential red phosphor for UV-white LED device, *J. Lumin.* 964 (2007) 122–123.
- [7] C. Chiu, M. Wang, C. Lee, T. Chen, Structural, spectroscopic and photoluminescence studies of  $\text{LiEu}(\text{WO}_4)_2 - x(\text{MoO}_4)_x$  as a near-UV convertible phosphor, *J. Solid. Stat. Chem.* 180 (2007) 619–627.

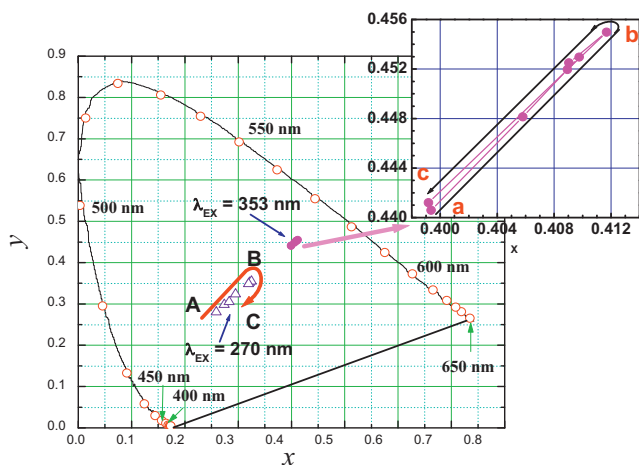


Fig. 11. CIE color coordinates for the phosphors with different concentrations of  $\text{Dy}^{3+}$ . (For interpretation of the references to color in this figure legend, the reader is referred to the web version of the article.)

- [8] K. Shinsho, Y. Suzuki, K. Harada, Y. Yamamoto, Multilevel based analysis of the thermoluminescence of  $\text{CaSO}_4\text{:RE}$  (RE = Tm, Dy, Tb, and Sm), *Appl. Phys. Lett.* 99 (2006) 043506–043514.
- [9] Y. Chen, C. Shi, W. Yan, Z. Qi, Y. Fu, Energy transfer between  $\text{Pr}^{3+}$  and  $\text{Mn}^{2+}$  in  $\text{SrB}_4\text{O}_7\text{:Pr, Mn}$ , *Appl. Phys. Lett.* 88 (2006) 061906–061909.
- [10] L. Cheng, X. Li, J. Sun, H. Zhong, Y. Tian, J. Wan, W. Lu, Y. Zheng, T. Yu, L. Huang, H. Yu, B. Chen, Investigation of the luminescence properties of  $\text{Dy}^{3+}$ -doped  $\text{a-Gd}_2(\text{MoO}_4)_3$  phosphors, *Physica B* 405 (2010) 4457–4461.
- [11] T.R.N. Kutty, Luminescence of  $\text{Ce}^{3+}$ -sensitized and  $\text{Dy}^{3+}$ -activated aluminoborates,  $\text{M}_3\text{Al}_6\text{B}_8\text{O}_{24}$  (M = Ca, Ba), *Mater. Res. Bull.* 25 (1990) 485–493.
- [12] Z. Pei, Q. Su, Y. Chui, J. Zhang, Investigation on the luminescence properties of  $\text{Dy}^{3+}$  and  $\text{Eu}^{3+}$  in  $\text{M}_3\text{Ln}_2(\text{B}_3\text{O}_3)_4$  (M = Ca, Sr, Ba; Ln = La, Gd, Y), *Mater. Res. Bull.* 26 (1991) 1059–1065.
- [13] Z. Pei, Q. Su, S. Li, Investigation on the luminescence properties of  $\text{Dy}^{3+}$  and  $\text{Eu}^{3+}$  in alkaline-earth borates, *J. Lumin.* 50 (1991) 123–126.
- [14] Y. Zhou, Z. Qiu, M. Lü, Q. Ma, A. Zhang, G. Zhou, H. Zhang, Z. Yang, Photoluminescence characteristics of pure and Dy-doped  $\text{ZnNb}_2\text{O}_6$  nanoparticles prepared by a combustion method, *J. Phys. Chem. C* 111 (2007) 10190–10193.
- [15] A.N. Belsky, N.M. Khaidukov, J.C. Krupa, V.N. Makhov, Philippov, Luminescence of  $\text{CsGd}_2\text{F}_7\text{:Er}^{3+}, \text{Dy}^{3+}$  under VUV excitation, *J. Lumin.* 94–95 (94) (2001) 45–50.
- [16] G.S.R. Raju, H.C. Jung, J.Y. Park, C.M. Kanamadi, B.K. Moon, J.H. Jeong, S. Son, J.H. Kim, Synthesis and luminescent properties of  $\text{Dy}^{3+}\text{:GAG}$  nanophosphors, *J. Alloys Compd.* 481 (2009) 807–811.
- [17] G.S.R. Raju, J.Y. Park, H.C. Jung, H.K. Yang, B.K. Moon, J.H. Jeong, J.H. Kim, Synthesis and luminescent properties of low concentration  $\text{Dy}^{3+}\text{:GAP}$  nanophosphors, *Opt. Mater.* 31 (2009) 1210–1214.
- [18] J. Kuang, Y. Liu, J. Zhang, White-light-emitting long-lasting phosphorescence in  $\text{Dy}^{3+}$ -doped  $\text{SrSiO}_3$ , *J. Solid State Chem.* 179 (2006) 266–269.
- [19] J.L. Sommerdijk, A. Bril, Efficiency of  $\text{Dy}^{3+}$ -activated phosphors, *J. Electrochem. Soc.* 122 (1975) 952–954.
- [20] H. Zhong, X. Li, R. Shen, J. Zhang, J. Sun, H. Zhong, L. Cheng, Y. Tian, B. Chen, Spectral and thermal properties of  $\text{Dy}^{3+}$ -doped  $\text{NaGdTiO}_4$  phosphors, *J. Alloys Compd.* 517 (2012) 170–175.
- [21] X. Yang, X. Yu, H. Yang, Y. Guo, Y. Zhou, The investigation of optical properties by doping halogen in the  $\text{BaMoO}_4\text{:Pr}^{3+}$  phosphor system, *J. Alloys Compd.* 479 (2009) 307–309.
- [22] J. Liao, B. Qiu, H. Lai, Synthesis and luminescence properties of  $\text{Tb}^{3+}\text{:NaGd}(\text{WO}_4)_2$  novel green phosphors, *J. Lumin.* 129 (2009) 668–671.
- [23] J. Liao, B. Qiu, H. Wen, J. Chen, W. You, Hydrothermal synthesis and photoluminescence of  $\text{SrWO}_4\text{:Tb}^{3+}$  novel green phosphor, *Mater. Res. Bull.* 44 (2009) 1863–1866.
- [24] N.S. Singh, R.S. Ningthoujam, M.N. Luwang, S.D. Singh, R.K. Vatsa, Luminescence, lifetime and quantum yield studies of  $\text{YVO}_4\text{:Ln}^{3+}$  ( $\text{Ln}^{3+} = \text{Dy}^{3+}, \text{Eu}^{3+}$ ) nanoparticles: concentration and annealing effects, *Chem. Phys. Lett.* 480 (2009) 237–242.
- [25] H. Ryu, K.S. Bartwal, Exploration and optimization of Dy codoping in polycrystalline  $\text{CaAl}_2\text{O}_4\text{:Eu}$ , *J. Alloys Compd.* 476 (2009) 379–382.
- [26] C. Chang, W. Li, X. Huang, Z. Wang, X. Chen, X. Qian, R. Guo, Y. Ding, D. Mao, Photoluminescence and afterglow behavior of  $\text{Eu}^{2+}, \text{Dy}^{3+}$  and  $\text{Eu}^{3+}, \text{Dy}^{3+}$  in  $\text{Sr}_3\text{Al}_2\text{O}_6$  matrix, *J. Lumin.* 130 (2010) 347–350.
- [27] J. Wan, L. Cheng, J. Sun, H. Zhong, X. Li, W. Lu, Y. Tian, H. Lin, B. Chen, Energy transfer and colorimetric properties of  $\text{Eu}^{3+}/\text{Dy}^{3+}$  co-doped  $\text{Gd}_2(\text{MoO}_4)_3$  phosphors, *J. Alloys Compd.* 496 (2010) 331–334.
- [28] M.M. Haque, H. Lee, D. Kim, Luminescent properties of  $\text{Eu}^{3+}$ -activated molybdate-based novel red-emitting phosphors for LEDs, *J. Alloys Compd.* 481 (2009) 792–796.
- [29] W. Kuang, Y. Fan, K. Yao, Y. Chen, Preparation, Characterization of ultrafine rare earth molybdenum complex oxide particles, *J. Solid State Chem.* 140 (1998) 354–360.
- [30] R.A. Rocha, E.N. Muccillo, Characterization of  $\text{La}_2\text{MoO}_6$  prepared by the cation complexation technique, *J. Alloy Comp.* 400 (2005) 83–87.
- [31] E. Sani, A. Toncelli, M. Tonelli, D.A. Lis, E.V. Zharikov, K.A. Subbotin, V.A. Smirnov, Effect of cerium codoping in  $\text{Er}^{3+}, \text{Ce}^{3+}\text{:NaLa}(\text{MoO}_4)_2$  crystals, *J. Appl. Phys.* 97 (2005) 123531–123537.
- [32] Y.C. Kang, M.A. Lim, H.D. Park, M. Han,  $\text{Ba}^{2+}$  Co-doped  $\text{Zn}_2\text{SiO}_4\text{:Mn}$  phosphor particles prepared by spray pyrolysis process, *J. Electrochem. Soc.* 150 (2003) H7–H11.
- [33] L. Zhang, H. Zhong, X. Li, L. Cheng, L. Yao, J. Sun, J. Zhang, R. Hua, B. Chen, Solid state reaction synthesis and luminescence properties of  $\text{Dy}^{3+}$ -doped  $\text{Gd}_2\text{Mo}_3\text{O}_9$  phosphor, *Physica B: Condens. Mater.* 407 (2012) 68–72.
- [34] L.G. Van Uitert, Characterization of energy transfer interactions between rare earth ions, *J. Electrochem. Soc.* 114 (1967) 1048–1053.
- [35] Y. Tian, B. Chen, B. Tian, R. Hua, J. Sun, L. Cheng, H. Zhong, X. Li, J. Zhang, Y. Zheng, T. Yu, L. Huang, Q. Meng, Concentration-dependent luminescence and energy transfer of flower-like  $\text{Y}_2(\text{MoO}_4)_3\text{:Dy}^{3+}$  phosphor, *J. Alloys Compd.* 509 (2011) 6096–6101.
- [36] M. Inokuti, F. Hirayama, Influence of energy transfer by the exchange mechanism on donor luminescence, *J. Chem. Phys.* 43 (1965) 1978–1989.